Lysophosphatidic acid targets vascular and oncogenic pathways via RAGE signaling

Vivek Rai,[1] Fatouma Touré,[1] Seth Chitayat,[2] Renjun Pei,[3] Fei Song,[1] Qing Li,[1] Jinghua Zhang,[1] Rosa Rosario,[1] Ravichandran Ramasamy,[1] Walter J. Chazin,[2] and Ann Marie Schmidt[1]

[1]Diabetes Research Program, Division of Endocrinology, Department of Medicine, New York University School of Medicine, New York, NY 10016
[2]Departments of Biochemistry and Chemistry and Center for Structural Biology, Vanderbilt University, Nashville, TN 37232
[3]Division of Clinical Pharmacology and Experimental Therapeutics, Department of Medicine, Columbia University Medical Center, New York, NY 10032

The endogenous phospholipid lysophosphatidic acid (LPA) regulates fundamental cellular processes such as proliferation, survival, motility, and invasion implicated in homeostatic and pathological conditions. Hence, delineation of the full range of molecular mechanisms by which LPA exerts its broad effects is essential. We report avid binding of LPA to the receptor for advanced glycation end products (RAGE), a member of the immunoglobulin superfamily, and mapping of the LPA binding site on this receptor. In vitro, RAGE was required for LPA-mediated signal transduction in vascular smooth muscle cells and C6 glioma cells, as well as proliferation and migration. In vivo, the administration of soluble RAGE or genetic deletion of *RAGE* mitigated LPA-stimulated vascular Akt signaling, autotaxin/LPA-driven phosphorylation of Akt and cyclin D1 in the mammary tissue of transgenic mice vulnerable to carcinogenesis, and ovarian tumor implantation and development. These findings identify novel roles for RAGE as a conduit for LPA signaling and suggest targeting LPA–RAGE interaction as a therapeutic strategy to modify the pathological actions of LPA.

CORRESPONDENCE
Ann Marie Schmidt:
annmarie.schmidt@nyumc.org
OR
Vivek Rai:
vivek.rai@nyumc.org

Abbreviations used: atx, autotaxin; DN, dominant negative; GPCR, G protein–coupled receptor; LPA, lysophosphatidic acid; MAP, mitogen-activated protein; MMTV, murine mammary tumor virus; POPC, 1-Palmitoyl-2-Oleoyl-*sn*-Glycero-3-Phosphocholine; RAGE, receptor for advanced glycation end products; S1P, sphingosine-1-phosphate; SMC, smooth muscle cell; SPR, surface plasmon resonance; sRAGE, soluble RAGE.

Endogenous phospholipids such as lysophosphatidic acid (LPA) regulate cellular signal transduction cascades implicated in diverse homeostatic and pathological conditions, from vascular signaling and tumorigenesis to neuropathic pain, as examples (Moolenaar et al., 2004; Lin et al., 2010). Thus, it is not surprising that the production of LPA is tightly regulated. The control of LPA levels occurs largely through the action of the enzyme autotaxin (atx), the principal source of LPA in the tissues (Georas, 2009; Pamuklar et al., 2009). In the vasculature and in tumors, LPA stimulates cellular proliferation, survival, motility, invasion, and production of growth factors (Moolenaar et al., 2004; Lin et al., 2010). LPA exerts homeostatic effects in development, but in adult organisms recrudescence of LPA signaling in stressed tissues is met with pathological responses such as neointimal expansion and tumor growth and metastasis (Moolenaar et al., 2004; Smyth et al., 2008; Lin et al., 2010). Although it is known that LPA interacts with G protein–coupled receptors (GPCRs), not all LPA activities can be explained by GPCR signaling. A potential role for an intracellular receptor has been proposed; further, unidentified LPA receptors or possibly nonreceptor pathways have been implicated in the biological actions of this lipid (McIntyre et al., 2003; Choi et al., 2010; Chun et al., 2010). Despite the high interest in LPA signaling, the identity of non-GPCR receptors has remained elusive. Because the receptor for advanced glycation end products (RAGE) has been implicated in vascular signaling, atherosclerosis, and tumorigenesis (Yan et al., 2010), we surmised that RAGE might mediate some of the biological effects of LPA and provide here substantial evidence in support of this hypothesis.

The Rockefeller University Press $30.00
J. Exp. Med. 2012 Vol. 209 No. 13 2339-2350
www.jem.org/cgi/doi/10.1084/jem.20120873

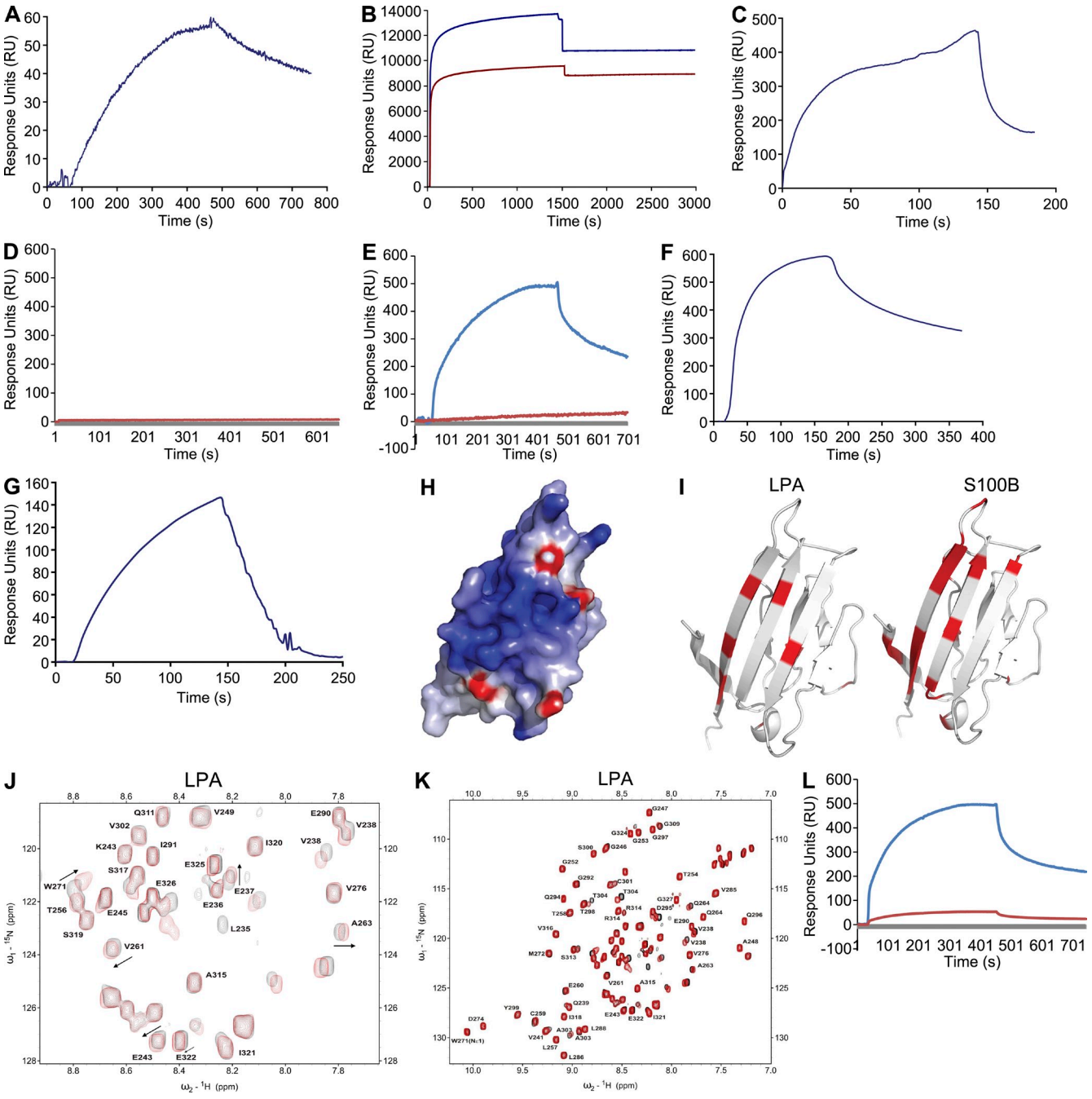

Figure 1. Direct binding of LPA to RAGE: SPR and NMR. (A) Binding of 218 nM LPA to the immobilized sRAGE surface on CM5 sensor chip and SPR sensorgrams. (B) A monolayer of POPC liposomes was formed on the flow cell 1 (dark blue), and a monolayer of LPA-POPC liposomes was formed on the flow cell 2 (dark red). (C) Binding of 4 nM sRAGE to the immobilized LPA surface on HPA sensor chip. (D) sRAGE does not bind to POPC liposomes immobilized on flow cell 1 HPA sensor chip in sRAGE-LPA binding experiment (red curve). (E) SPR sensorgrams indicating that 1 µM sRAGE does not interact with immobilized S1P-POPC surface on flow cell 2 of the HPA sensor chip (dark red) and that sRAGE binds to LPA on flow cell 1 immobilized with LPA-POPC as the positive control for binding interaction (blue curve). (F) Binding of 9 nM RAGE V domain to the immobilized LPA surface. (G) Binding of 1 µM RAGE C2 domain to the immobilized LPA surface on HPA sensor chip. (H) Surface representation of the V domain (PDB 3CJJ) colored by electrostatic field, showing the highly basic (blue) character of the LPA binding surface. (I) NMR chemical shift perturbations mapped on the structure of the V domain (PDB 3CJJ) for LPA and Ca^{2+}-loaded S100B. The significantly perturbed residues are highlighted in red. (J) ^{15}N-^{1}H HSQC NMR spectrum of ^{15}N-enriched C2 domain in the absence (black) and presence (red) of LPA. (K) Complete ^{15}N-^{1}H HSQC NMR spectrum of ^{15}N-enriched C2 domain in the absence (black) and presence (red) of LPA. (L) Binding of 1 µM sRAGE with 1 µM BSA or 1 µM S100B to the immobilized LPA liposomes on HPA sensor chip (blue and red, respectively). SPR assays results shown are representative of three independent experiments.

Table 1. RAGE binds LPA: data analysis from Biacore studies

Experiment	k_a (association rate)	k_d (dissociation rate)	Rmax	K_D
	1/Ms	*1/s*	*RU*	*M*
LPA to immobilized sRAGE	1.06×10^4	9.00×10^{-4}	56	8.49×10^{-8}
sRAGE to LPA liposomes	1.96×10^7	0.03	356	1.36×10^{-9}
V domain RAGE to LPA liposomes	1.72×10^7	0.04	467	2.47×10^{-9}
C2 domain to LPA liposomes	1.95×10^4	0.01	146	6.35×10^{-6}

RESULTS AND DISCUSSION

LPA binds to RAGE primarily through RAGE V-type immunoglobulin domain

To test the hypothesis that LPA could induce signaling through RAGE, we first performed experiments to test for LPA–RAGE physical interaction. The extracellular portion of RAGE (soluble RAGE [sRAGE]) was immobilized on a carboxymethylated dextran CM5 chip and high affinity LPA binding was observed by surface plasmon resonance (SPR; Fig. 1 A). To confirm the interaction, we reversed the binding assay and examined the binding of sRAGE to immobilized LPA (18:1) 1-Palmitoyl-2-Oleoyl-*sn*-Glycero-3-Phosphocholine (POPC; POPC-LPA 10:1 wt/wt) and POPC liposomes as a reference on the HPA sensor chip (Fig. 1 B). The SPR binding response in these experiments validated that sRAGE bound LPA (Fig. 1 C).

We next asked if distinct lipids bound to RAGE. POPC, a member of the phosphatidylcholine family of lipids, was used as a negative control (HPA chip flow cell 1) in the Biacore SPR assay and did not bind RAGE (Fig. 1 D). Furthermore, we tested the sphingolipid sphingosine-1-phosphate (S1P). As shown in Fig. 1 E (red curve), S1P did not bind to RAGE with appreciable affinity. In Fig. 1 E, the blue curve represents positive control sRAGE-LPA binding.

It has been reported that ligand binding to RAGE occurs through the extracellular N-terminal V-type immunoglobulin domain that is part of the extracellular VC1 structural module and possibly through the C2 domain (Leclerc et al., 2007). To understand the mechanism by which RAGE binds LPA, the LPA-modified surface was used in SPR experiments to further probe the binding of LPA to sRAGE using the isolated V domain and C2 domains. We observed high affinity binding of LPA to V domain with a dissociation constant of (K_d) of 9×10^{-9} M (Fig. 1 F), nearly the same as that to full-length sRAGE. The interaction of the C2 domain to an LPA-modified surface was 1,000-fold weaker with the estimated Kd of 9×10^{-6} M (Fig. 1 G). Table 1 lists the association and dissociation rates, and the Rmax and K_D values for each of the above experiments.

Next, to confirm that LPA binds directly to RAGE, heteronuclear NMR experiments were performed using samples of ^{15}N-enriched V and C2 domains. Titrations of the V domain with LPA resulted in selective broadening of the NMR signals. The residues most perturbed by the addition of LPA include Lys52, Val63, Trp72, Gly90, Gln100, Lys110, Tyr113, and Val115, which map to a specific basic surface on the V domain structure (Fig. 1 H) that is a logical site for interaction of negatively charged LPA. Previous work by our group and others has identified this surface as the site for binding the endogenous RAGE ligands S100B and AGE (Fig. 1 I; Dattilo et al., 2007; Koch et al., 2010; Xue et al., 2011). In the titration of the C2 domain with LPA, a limited number of resonances exhibited perturbations in the intermediate to fast exchange regimen on the NMR timescale (Fig. 1, J and K). These observations indicate that LPA physically interacts with RAGE; the interaction of the C2 domain with LPA is significantly weaker than that observed for the V domain and is consistent with the 1,000-fold weaker binding reported by SPR. To further investigate where LPA binds on RAGE, the SPR assay for binding to LPA was performed with preincubation of sRAGE with BSA (Fig. 1 L, blue curve) or S100B (Fig. 1 L, red curve). The observed suppression of LPA interaction by S100B, but not BSA, confirms that the two ligands bind to the same site on RAGE.

LPA-mediated Akt signal transduction in primary murine aortic smooth muscle cells (SMCs) requires RAGE

Based on these data, we tested the hypothesis that LPA initiates signal transduction through RAGE. As the full repertoire of LPA receptors in SMCs is not fully clarified (Kim et al., 2006; Panchatcharam et al., 2008), we performed experiments in primary murine aortic SMCs from wild-type and RAGE-null mice. Activation of Akt and ERK was determined in wild-type and RAGE-null SMCs in response to LPA. We first performed a dose response study and found significant activation of Akt in SMCs treated with 1, 10, or 20 μM LPA (Fig. 2 A). We used a dose of 10 μM for all subsequent studies. Although LPA treatment activated Akt in wild-type SMCs, LPA-stimulated activation of Akt was not observed in RAGE-null SMCs (Fig. 2 B). In contrast, LPA-stimulated ERK phosphorylation and the degree of activation did not differ between wild-type and RAGE-null SMCs (Fig. 2 C). These data suggest that there are distinct functional receptors for LPA on SMCs, and that RAGE mediates the effects of LPA through Akt, but not ERK signal transduction.

Consistent with the binding of LPA to RAGE, equimolar concentrations of sRAGE blocked LPA-mediated phosphorylation of Akt in SMCs (Fig. 2 D). We performed gain- and loss-of-function experiments in wild-type and RAGE-null SMCs. We transiently transfected wild-type SMCs with full-length

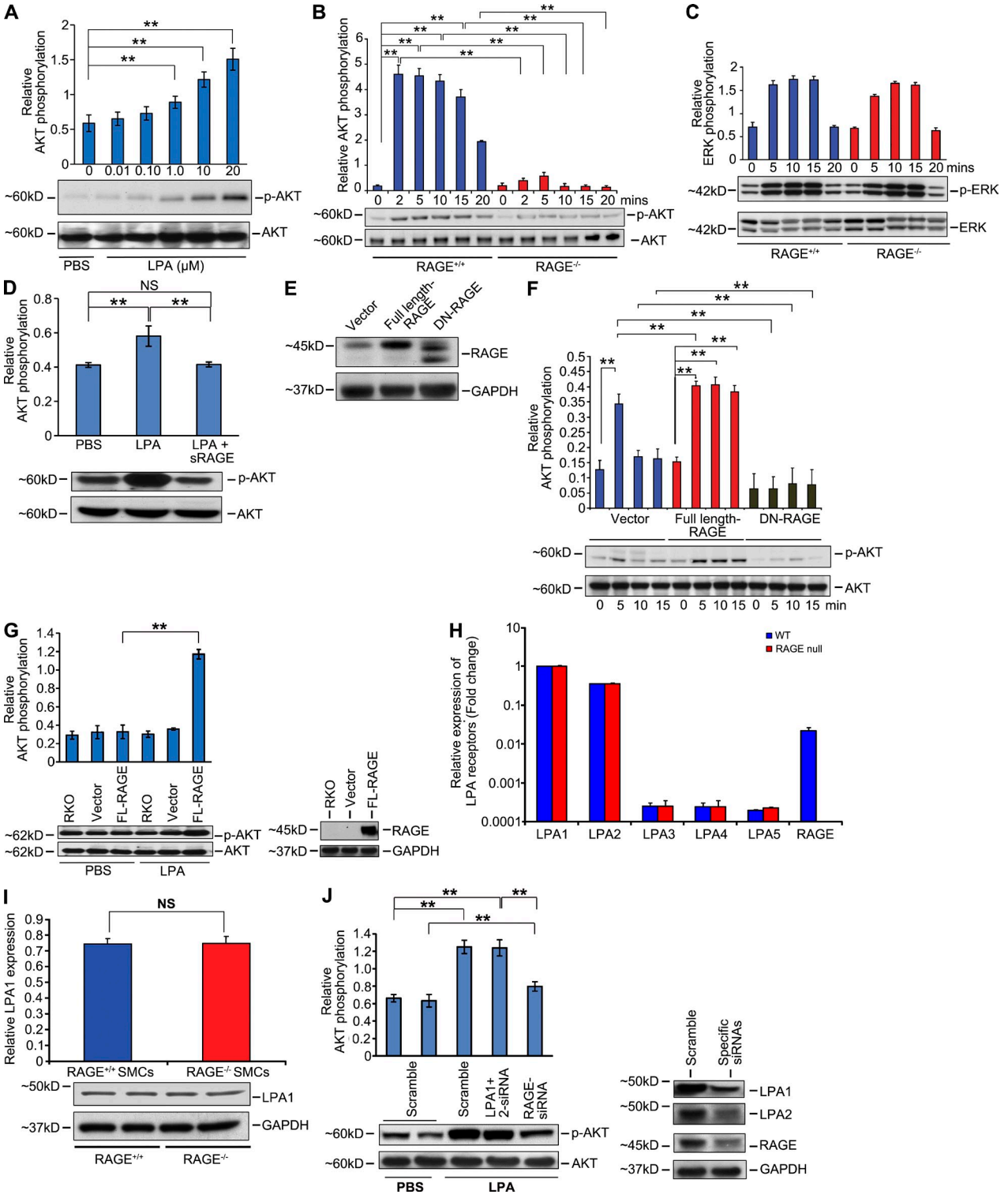

Figure 2. RAGE is a functional LPA receptor in vascular SMCs. (A) Quantified levels of phosphorylated/total AKT are shown in wild-type and RAGE-null SMCs, upon 0 to 0.01–20 μM LPA stimulation. (B and C) Quantified levels of phosphorylated/total AKT (B) and ERK (C) are shown in wild-type and RAGE-null SMCs, upon 10 μM LPA stimulation at the indicated times. (D–G) Quantified levels of phosphorylated/total AKT induced by LPA were tested in the presence of sRAGE (D), in the presence of SMCs transfected with control vector, full-length RAGE or DN RAGE (E and F), or in RAGE-null SMCs transfected with vector, or full-length RAGE (G). In E, RAGE levels are shown by Western blotting in transfected SMCs and, after probing with the primary anti-RAGE antibody, blots were stripped and reprobed with antibody to GAPDH. (H) Real time PCR for LPA receptors 1–5 and RAGE gene products was performed, normalized to 18s transcript levels, and expressed as fold change comparing wild-type versus RAGE-null SMCs. (I) LPA1 receptor levels as

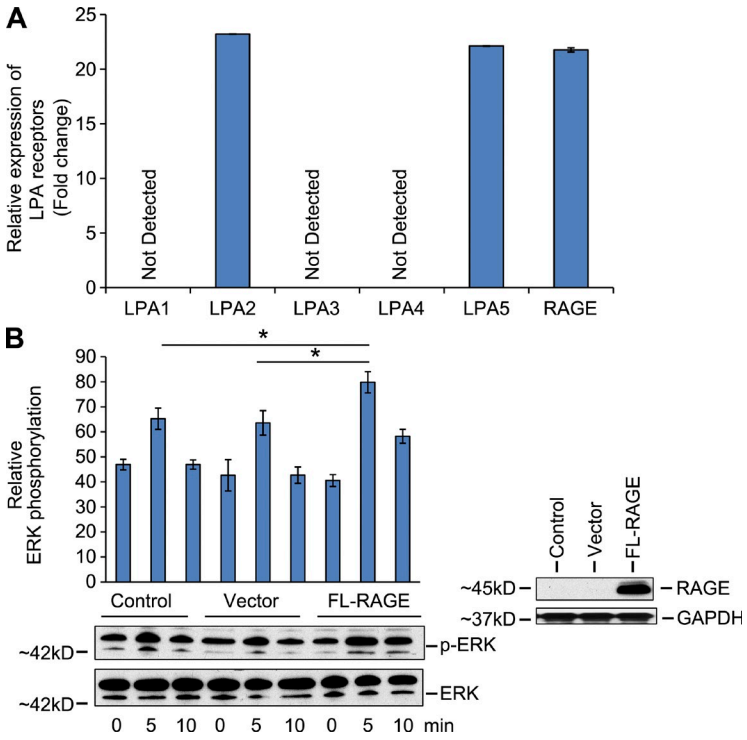

Figure 3. RAGE activates ERK in RH-7777 in rat hepatoma cells. (A) Real-time PCR for LPA receptors 1–5 and RAGE mRNA transcripts was performed in RH-7777 cells and normalized to 18s transcript levels. The graphs show relative fold of LPA receptor transcripts in RH-7777 cells. Assays were performed in triplicate and results shown are representative of two independent experiments. (B) Quantified levels of phosphorylated/total ERK are shown in RH-7777 rat hepatoma cells transfected with control vector, full-length RAGE, and upon 10 µM LPA stimulation at the indicated times. Representative results from triplicate experiments and at least two independent experiments are shown. *, $P < 0.05$. Error bars represent SD.

RAGE or signaling-deficient, cytoplasmic domain–deleted dominant-negative (DN) RAGE (Fig. 2 E). LPA induced robust phosphorylation of Akt in RAGE-overexpressing SMCs compared with vector but failed to induce Akt phosphorylation in SMCs expressing DN-RAGE (Fig. 2 F). Transfection of RAGE-null SMCs with RAGE-expressing vector restored LPA-mediated phosphorylation of Akt compared with untransfected or vector-transfected SMCs (Fig. 2 G).

Next, to be certain that RAGE deletion did not impact the expression of the major LPA receptors of the GPCR family in SMCs, we determined the transcript levels for these receptors in both wild-type and RAGE-null SMCs (Fig. 2 H) and assessed protein expression of LPA1 receptor and its potential dependence on RAGE (Fig. 2 I). We found that LPA1, LPA2, and RAGE were the main LPA receptors on SMCs and that deletion of RAGE did not impact expression levels of LPA1-5. To determine the role of RAGE in LPA-mediated activation of Akt in SMCs, we used siRNA to reduce expression of LPA1+2 or RAGE in these cells. Knockdown of LPA1+2 had no effect on LPA-mediated activation of Akt, but knockdown of RAGE significantly reduced LPA-stimulated Akt phosphorylation (Fig. 2 J).

In addition, we tested RH7777 cells, as these cells are devoid of most LPA receptors (Valentine et al., 2008). As shown in Fig. 3 A only LPA2, LPA5, and RAGE, but not LPA1, LPA3, or LPA4 are expressed in these cells as shown by quantitative real-time PCR. When we overexpressed full-length RAGE in these cells, we found that stimulation with LPA resulted in a significantly higher degree of ERK phosphorylation compared with treatment of control or vector control-transfected cells (Fig. 3 B). Hence, in the presence of only two non-RAGE LPA receptors (LPA2 and LPA5), overexpression of RAGE augmented LPA-dependent signaling.

RAGE-dependent vascular signaling: in vivo studies

To test if LPA serves as a RAGE ligand in vascular cells in vivo, LPA was infused into the left ventricles of wild-type and RAGE-null mice and activation of Akt was tested. In wild-type mice, LPA induced rapid (15 min) activation of Akt in vivo in SMCs as revealed by immunostaining of aorta tissue sections and Western blotting for detection of phospho-Akt. In contrast, RAGE-null mice displayed significantly less Akt phosphorylation in the aorta after administration of LPA (Fig. 4, A and B). Note that studies at later time points (30 and 60 min after LPA infusion) revealed that Akt phosphorylation was not simply delayed in RAGE-null mice, as there was no increase in pAkt/total Akt in either wild-type or RAGE-null mice after LPA infusion at 30 or 60 min after LPA infusion (Fig. 4 B).

shown by Western blotting in wild-type and RAGE-null SMCs. After probing with the primary anti-LPA1 antibody, blots were stripped and reprobed with antibody to GAPDH. NS, not significant. (J) Transiently transfected scramble control (PBS) or scramble, LPA_1 + LPA_2 siRNAs, or RAGE siRNA–transfected primary murine aortic SMCs were stimulated with 10 µM LPA. Total lysates were subjected to Western blotting with antibodies against total AKT or p-AKT. Quantified levels of phosphorylated/total Akt in the wild-type–transfected SMCs are shown (fold changes are relative to control). **, $P < 0.05$. Assays results shown are representative of three independent experiments. Error bars represent SD.

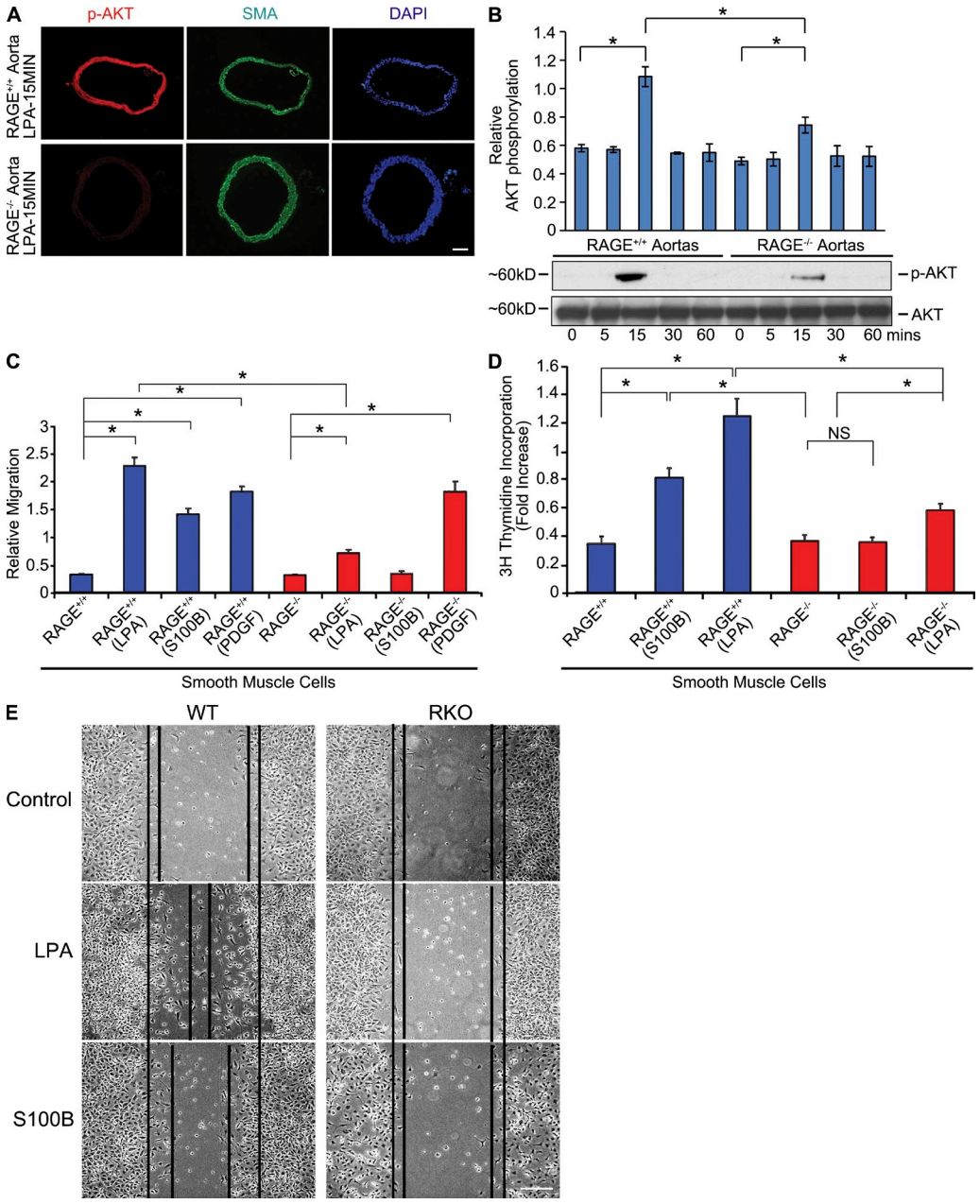

Figure 4. LPA infusion into mouse hearts activates Akt signal transduction via RAGE. (A) LPA (200 µl of a 100 µM solution) was infused directly into wild-type and RAGE-null mice left ventricles. Aortas were retrieved and confocal microscopy was performed on aortic tissue and subjected to immunostaining for detection for p-Akt (15 min). The left column reveals staining with a p-Akt-specific antibody; the middle column reveals staining with monoclonal mouse smooth muscle actin antibody specific to SMC-actin; and the right column reveals the DAPI staining for nuclei. Bar, 100 µm. (B) Mice aortas were retrieved at the indicated times, lysed, and LPA-induced Akt phosphorylation was determined by Western blotting. (C and D) Wild-type and RAGE-null SMCs were treated with 10 µM LPA, 10 µg/ml S100B, or 10 ng/ml platelet-derived growth factor (PDGF) for 5 or 48 h, and migration (C) and proliferation (D), respectively, were assessed. Error bars represent SD. Assays were performed in triplicate and results are representative of three independent experiments. (E) Serum-starved RAGE-expressing SMCs and RAGE-null SMCs were scratched and treated with 10 µM LPA or 10 µg/ml S100B for 18-h LPA-stimulated wound healing in RAGE-expressing SMCs but not in RAGE-null SMCs. RAGE ligand S100B was used as reference. Bar, 100 µm. Assays were performed in triplicate and results are representative of three independent experiments. *, $P < 0.005$.

LPA displays chemoattractant effects in vascular SMCs (Panchatcharam et al., 2008; Smyth et al., 2008). To specifically test if RAGE contributed to LPA-mediated SMC migration and proliferation, we performed studies in SMCs retrieved from RAGE-expressing or RAGE-null mouse aortas. Migration and proliferation responses to LPA in RAGE-null SMCs were significantly lower than those observed in wild-type SMCs (Fig. 4, C and D, respectively).

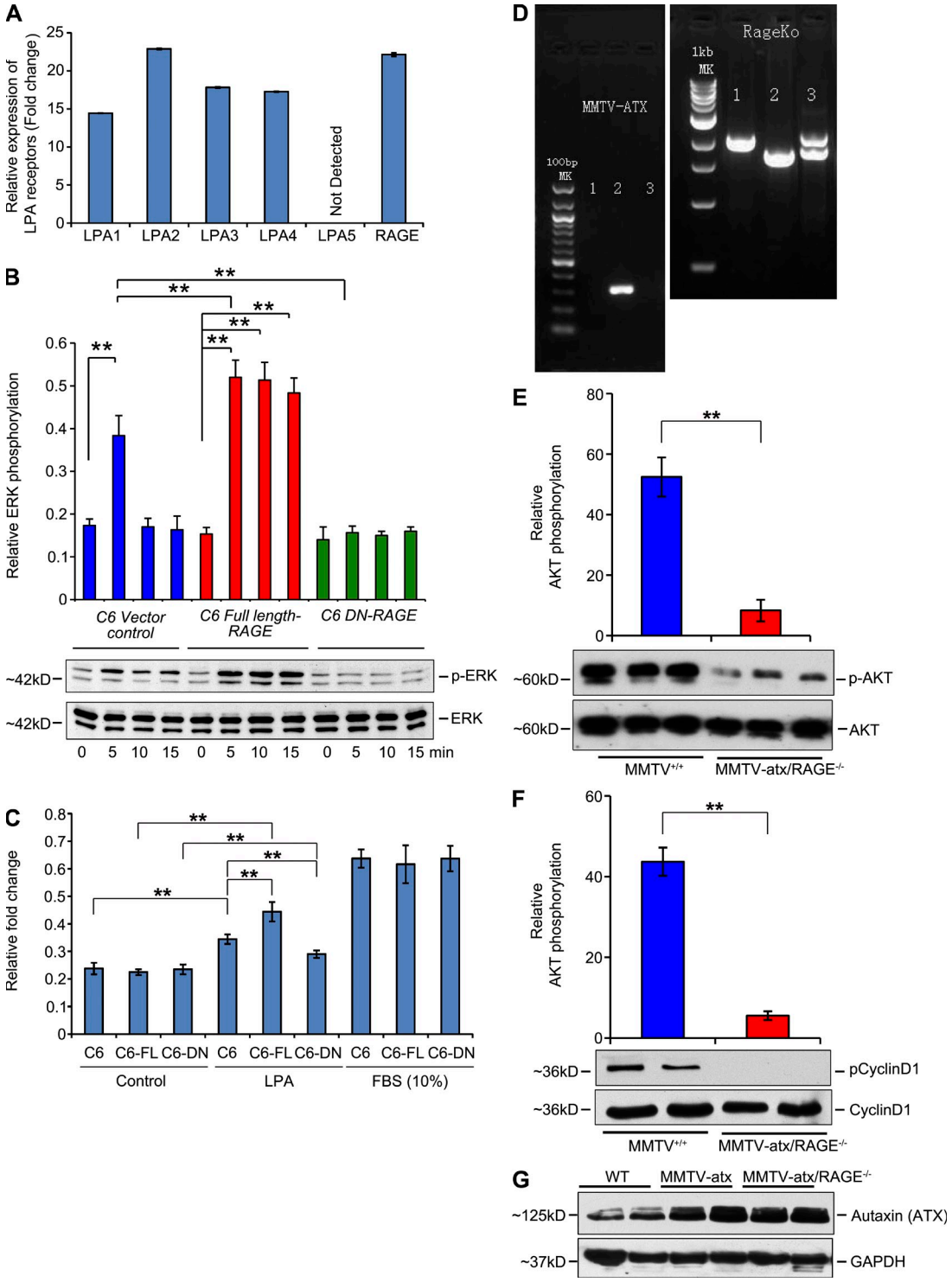

Figure 5. RAGE is a functional LPA receptor on C6 glioma tumor cells and is required for atx/LPA–mediated signaling in vivo. (A) Relative expression of transcripts of LPA receptors. Real-time PCR for LPA receptors 1–5 and RAGE gene products was performed, normalized to 18s transcript levels, and expressed as fold change in C6 glioma cells. The graphs show relative fold of LPA receptor transcripts. Assays were performed in triplicate and results are representative of two independent experiments. Error bars represent SD. (B) Quantified levels of phosphorylated/total ERK in the C6, C6 full-length RAGE, and C6 DN-RAGE cells upon LPA stimulation (10 µM) at different times, determined by Western blotting are shown. Fold changes are relative to control. (C) Colony-forming unit assays were performed in C6 glioma cells in the presence of control vector, full-length RAGE, or DN RAGE in the presence of 10 µM LPA or fetal bovine serum (10%). In B and C, ** indicates $P < 0.05$. Assays were performed and results are representative of three (B) and two (C) independent experiments. Error bars represent SD. (D–G) MMTV-*atx* mice were bred into the RAGE-null background and these mice and littermate

Similar patterns of migration and proliferation were noted in SMCs exposed to a distinct RAGE ligand, S100B (Fig. 4, C and D). However, incubation of SMCs with a non-RAGE ligand, PDGF, mediated comparable degrees of cellular migration in both wild-type and RAGE-null SMCs (Fig. 4 C). In addition, experiments in SMC wound healing assays confirmed roles for RAGE in LPA signaling (Fig. 4 E).

LPA–RAGE interaction mediates C6 glioma tumor cell phosphorylation of ERK mitogen-activated protein (MAP) kinase

As it was essential to test the role of RAGE in transducing the effects of LPA in a distinct cell type to support our hypothesis, and because LPA and RAGE play key roles in the behavior of transformed cells, additional experiments were performed using C6 glioma cells stably expressing vector control, full-length RAGE, or DN-RAGE (Taguchi et al., 2000). These cells express LPA1, LPA2, LPA3, and LPA4 receptors in addition to RAGE (Fig. 5 A), so our experiments were specifically designed to obtain evidence of signaling through RAGE. Activation of ERK MAP kinase is stimulated by LPA in C6 glioma cells (Cechin et al., 2005). C6 glioma cells stably expressing full-length RAGE revealed strong phosphorylation of ERK in response to LPA over 15-min stimulation, which was greater than that seen in vector alone cells (Fig. 5 B). In contrast, LPA-stimulated ERK phosphorylation was not detected in stably expressing DN-RAGE C6 cells (Fig. 5 B). We next performed colony-forming assays and show that compared with vector control C6 glioma cells, LPA induced a significant increase in colony-forming units in full-length RAGE-overexpressing cells. Furthermore, colony forming units were greatly reduced in the presence of DN-RAGE (Fig. 5 C). In contrast, exposure of C6 glioma cells to a general stimulus, fetal bovine serum (10%), stimulated colony-forming units in a manner independent of RAGE overexpression or DN-RAGE (Fig. 5 C).

Role for RAGE in atx/LPA-mediated signaling in a murine model of mammary tumor development

In the above studies, we stimulated cells and animals exogenously with LPA. To test if RAGE transduced the signals stimulated by endogenously produced LPA, we used transgenic mice overexpressing atx under the control of the murine mammary tumor virus (MMTV) LTR promoter, which enables control of the levels of LPA. Hence, LPA is produced endogenously in these mice. In the mammary tissues of MMTV-*atx* mice, phosphorylation of Akt and hyperplasia were previously shown to be significantly higher versus that observed in control wild-type mice of the FVB background (Liu et al., 2009). To test the impact of RAGE, we bred MMTV-*atx* mice into the RAGE-null background and compared findings to those observed in littermate MMTV-*atx* mice expressing RAGE, all in the FVB background (Fig. 5 D). Mammary glands were retrieved from female animals at age 6 wk to determine the effects of RAGE deletion on modulation of early signal transduction pathways implicated in tumor development (Liu et al., 2009). Compared with MMTV-*atx* mice expressing RAGE, mammary glands retrieved from those mice devoid of RAGE revealed significantly less phosphorylation of Akt (Fig. 5 E) and phosphorylation of cyclin D1 (Fig. 5 F). Note that levels of atx in the mammary tissue did not differ between MMTV-*atx* mice expressing RAGE versus MMTV-*atx* mice devoid of RAGE (Fig. 5 G).

Blockade or genetic deletion of RAGE suppresses LPA-mediated tumor formation in vivo

As it is established that LPA enhances tumor implantation and metastasis of ID8 cells, a murine epithelial ovarian cancer cell line (Roby et al., 2000; Li et al., 2009), in immunocompetent C57BL/6 mice, we tested if there is a role played by RAGE. ID8 cells express RAGE (Fig. 6 A). When ID8 cells are injected by intraperitoneal administration, near complete dependence on LPA treatment to stimulate tumor growth and metastasis has been observed (Li et al., 2009). Daily injections of LPA versus PBS alone for 4 wk enhanced tumor implantation from ID8 cells in RAGE-expressing wild-type mice (Fig. 6, C vs. B, respectively, and G). Tumors were present on the peritoneal wall, diaphragm, omentum, and mesentery, and on the surface of the spleen, liver, kidney, and small intestine.

To test the effect of RAGE, we used sRAGE and RAGE-null mice. LPA-induced tumor numbers were significantly reduced in sRAGE-treated wild-type and RAGE-null groups (Fig. 6, D, F, and G). Thus, sRAGE and RAGE deficiency significantly affected LPA-induced tumor implantation and metastasis. The representative hematoxylin and eosin (H&E) staining of the tumors from all groups is shown in Fig. 6, H–L.

Based on comprehensive physicochemical and biological experimentation in vitro, in cellular systems, and in vivo, we identify RAGE as a previously unrecognized receptor for LPA and illustrate the complex signaling network induced by this biologically active phospholipid. Although a role for the strongly positive electrostatic potential at the ligand binding surface of RAGE is clearly evident, the mechanism of activation by the diverse chemical structures of the various RAGE

RAGE-expressing MMTV-*atx* mice were studied. (D) Genotyping of MMTV-*atx* and RAGE mice. Left panel shows the genotyping of MMTV-*atx* mice; PCR was performed according to established protocols. Right panel shows the genotyping of RAGE-expressing (+/+), heterozygous (+/−), and null (−/−) mice using protocols established in our laboratory. Note that Mouse #2 for example is an MMTV-*atx*+ (hemizygous)/RAGE-null mouse used in the studies. (E and F) At 6 wk of age, mammary tissue was retrieved and subjected to Western blotting for detection of phosphorylated/total Akt and phosphorylated/total cyclin D1. n = at least 3 replicates per group; **, $P < 0.005$. Error bars represent SD. (G) Mammary tissue from wild-type, MMTV-*atx*/RAGE–expressing mice, and MMTV-*atx*/RAGE-null mice was retrieved at age 6 wk and subjected to Western blotting for detection of atx. $n = 3$ mice per group.

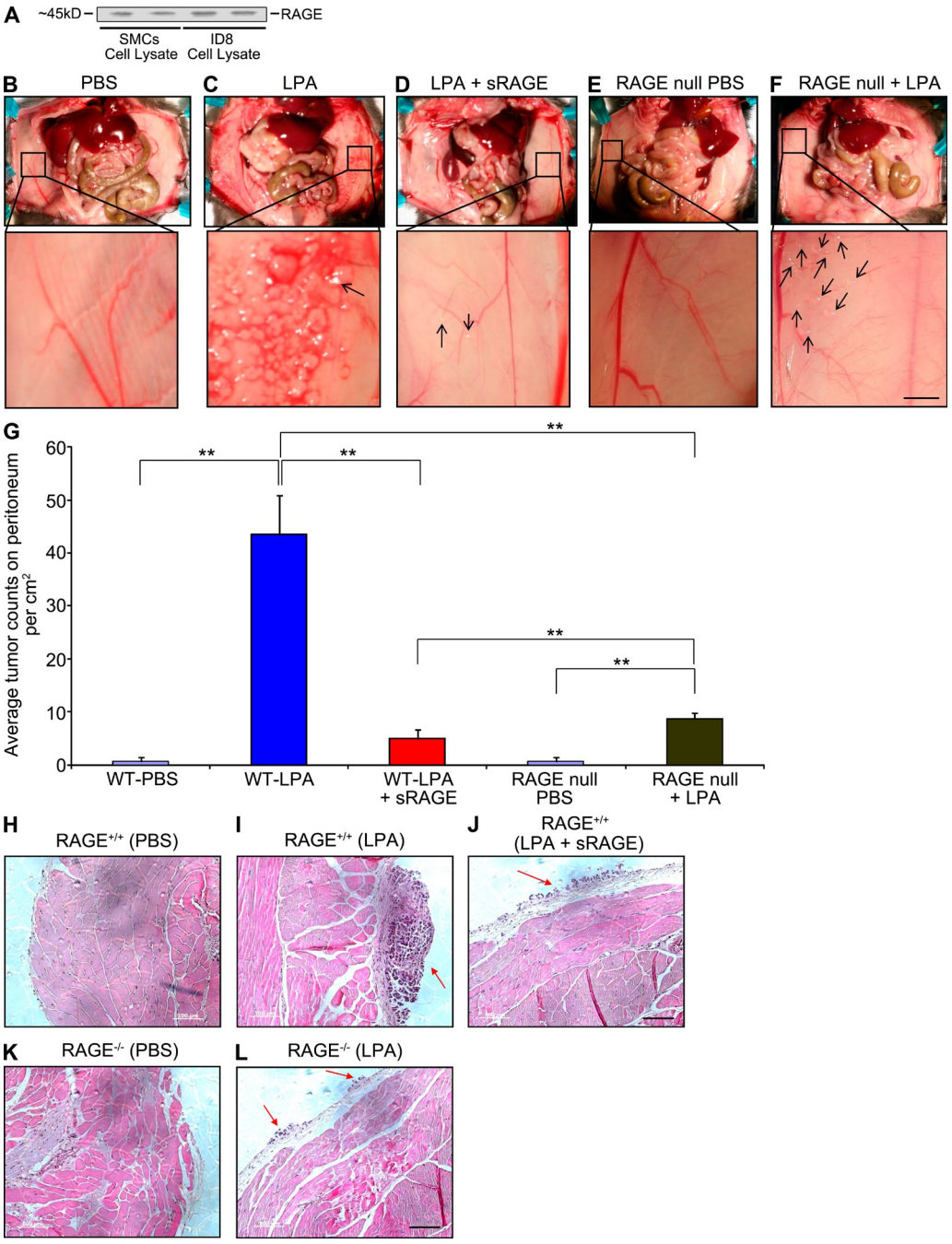

Figure 6. RAGE is a functional LPA receptor: RAGE deletion and sRAGE block LPA–induced growth of implanted ID8 tumor cells. (A) RAGE expression is shown by Western blotting in ID8 ovarian cancer cells probing with the primary anti-RAGE antibody in murine SMC lysates (lanes 1 and 2) and murine ID8 cells (lanes 3 and 4). Assays were performed in triplicate and results are representative of two independent experiments. (B–L) ID8 ovarian cancer cells were implanted into immunocompetent wild-type mice receiving PBS (B), wild-type mice receiving LPA (C), wild-type mice receiving LPA and sRAGE (D), RAGE-null mice receiving PBS (E), and RAGE-null mice receiving LPA (F), and tumor numbers/cm^2 on day 28 are shown, $n = 5$ per group (G). The dose of LPA was 200 µl of a 100 µM solution given per day. sRAGE (200 µl of a 50 µM solution/day for 28 d) was administered to mice in F. Bar, 3 mm. (H–L) Representative H&E stained images of tumors retrieved from the peritoneal cavity on day 28 of mice bearing ID8 cells tumors after the indicated treatments are shown. Bar, 100 µm. Error bars represent SD. **, $P < 0.05$.

ligands remains enigmatic. We do note, however, that our data reveal that RAGE does not bind POPC or S1P. Furthermore, although RAGE ligands are chemically distinct, virtually all are produced in the process of damage and stress within the cellular microenvironment. Moreover, as shown elsewhere for other RAGE ligands and here for LPA, there is

a distinct specificity within each class of ligands. Potent roles for RAGE have been demonstrated in multiple facets of chronic inflammatory diseases such as diabetes, atherosclerosis, and tumorigenesis (Park et al., 1998; Hofmann et al., 1999; Taguchi et al., 2000; Sakaguchi et al., 2003; Zhou et al., 2003; Chen et al., 2004; Bu et al., 2010). The finding that LPA is a functional ligand for RAGE expands this repertoire of RAGE ligand families and sheds new light on settings in which LPA may contribute to disease pathogenesis.

We recently discovered that the cytoplasmic domain of RAGE binds to the formin mammalian diaphanous-1 (mDia1); in transformed cells, macrophages, and SMCs, mDia1 is essential for RAGE ligand (AGE and S100B)–mediated activation of Rho GTPases and downstream signal transduction, formation of lamellipodia, and cellular migration (Hudson et al., 2008; Xu et al., 2010; Touré et al., 2012). Indeed, it has been shown that LPA regulates cellular morphology and invasion in transformed cells and fibroblasts via a mechanism requiring mDia1 through signaling cascades including GSK-3β (Copeland and Treisman, 2002; Eng, et al., 2006; Kitzing, et al., 2007). Our recent work illustrates that SMC migration induced by S100B-RAGE signaling via mDia1 requires serine 9 phosphorylation of GSK-3β (Touré et al., 2012) and the ROCK signaling pathway (Bu et al., 2010). In this context, it is important to note that in distinct cells—adult murine cardiomyocytes—RAGE ligands result in reduced serine 9 phosphorylation of GSK-3β (Shang, et al., 2010), thereby highlighting the cell-type specificity of RAGE signals. Collectively, these considerations provide a logical link to the biology of LPA and support integral roles for RAGE in transducing LPA-mediated signal transduction.

Previously reported LPA receptors are members of the GPCR family; thus, our studies identify a unique receptor of the immunoglobulin superfamily active in transducing LPA's biological effects. Whether or not these receptor families function alone or in concert, and what are their precise mechanisms of action, remain important questions that must be addressed in future studies. We conclude that optimal therapeutic strategies in vascular disease and tumors might include targeting LPA/RAGE-stimulated signal transduction.

MATERIALS AND METHODS

sRAGE, V domain, and C2 domain: expression and purification. Human sRAGE, V domain, and C2 domain proteins were expressed and purified as previously described (Park et al., 1998; Dattilo et al., 2007).

LPA and LPA liposomes. 18:1 LPA, 18:1 Lyso PA 1-oleoyl-2-hydroxy-sn-glycero-3-phosphate (sodium salt), and S1P (d18:1) were purchased from Avanti Polar Lipids, Inc. The 100-nm-size LPA-POPC (1:10, wt/wt) liposomes, S1P-POPC (1:10, wt/wt), and POPC liposomes were purchased from Encapsula Nanosciences.

SPR experiments. All experiments were performed at 25°C using a Biacore X with commercially available Biacore CM5 sensor chips or HPA sensor chips (GE Healthcare). HBS buffer (10 mM Hepes, pH 7.4, and 150 mM NaCl) was used as running buffer. Proteins were immobilized on the carboxymethyl dextran surface of flow cell 2 using amine-coupling chemistry with a flow rate of 5 µl/min. Flow cell 1 remained unmodified to serve as a reference cell for the subtraction of systematic instrument noise and drift. LPA was immobilized on the HPA sensor chip by solubilization in LPA liposomes.

LPA binding to the sRAGE immobilized surface. The carboxyl groups on the CM5 sensor chips were activated for 7 min using 0.1 M N-hydroxysuccinimide and 0.4 M (N-ethyl-N′-3-dimethylaminopropyl) carbodiimide mixed at 1:1 (vol/vol) ratio. In the coupling step, a 30 µl injection of 0.16 mg/ml sRAGE (in sodium acetate buffer, pH 5.5) was flowed over the activated surface for 6 min. The remaining activated sites on the chip surfaces were blocked with a 35 µl injection of an ethanolamine hydrochloride solution (1 M, pH 8.5), followed by a 60-s wash with 2 M NaCl to remove any nonspecifically adsorbed materials. About 4,000 RU of the immobilized sRAGE proteins was obtained.

LPA dilutions were prepared in HBS buffer and injected sequentially over two flow cells at a flow rate of 10 µl/min. Surface regeneration was achieved using a 60-s injection of 2 M NaCl. The response curve was obtained by subtraction of the signals over the reference surface from the binding response over RAGE immobilized surface.

sRAGE and domains binding to LPA immobilized surface. LPA liposomes were used to generate a stable mimic membrane on the HPA sensor surfaces. The 18:1 LPA, LPA-POPC (1:10, wt/wt) liposomes, S1P-POPC (1:10, wt/wt), and POPC liposomes were obtained from Encapsula Nanosciences. The chips were cleaned by washing with octyl glucoside for 1 min at 10 µl/min, and 0.5 mM liposomes as prepared above were passed over the flow cells for 25 min at 4 µl/min. The chips were washed with a 30-s injection of 50 mM sodium hydroxide twice to remove the loosely bound liposomes to obtain stable base line. In a typical experiment, a monolayer of POPC was deposited in flow cell 1 and referred to as POPC surface. A monolayer of LPA-POPC or S1P-POPC was deposited in flow cell 2 and referred to as LPA-POPC or S1P-POPC surface.

The dilutions of sRAGE, V domain, and C2 domain were prepared in HBS buffer and injected sequentially over two flow cells at a flow rate of 30 µl/min for 150 s. The response curves were obtained by subtraction of the response signals over POPC surface from the binding response over LPA-POPC surface and were analyzed using Biacore software.

NMR binding studies. Experiments were performed at 25°C on a Bruker DRX500 spectrometer equipped with a Z-axis gradient cryoprobe. LPA was titrated into a solution of 50 µM ^{15}N-labeled V domain in 20 mM phosphate, pH 6.0, and perturbations in NMR signals were monitored by acquiring 2D ^{15}N-^{1}H HSQC spectra. The corresponding experiments for C2 were performed in 20 mM phosphate, pH 6.1. Acquired data were processed using Topspin 2.1 (Bruker) and analyzed using NMRViewJ. The ratios of intensities between spectra with and without LPA (I/Io) were calculated for all well resolved resonances. Chemical shift perturbations were measured using the equation $\Delta\delta = [(0.17\Delta\delta_N)^2 + (\Delta\delta_{HN})^2]^{1/2}$.

Cell lines and materials. Wild-type and RAGE-null primary murine aortic vascular SMCs were isolated and used through passage 5 to 7. Rat C6 glioma cells and McA-RH7777 rat hepatoma cells were obtained from American Type Culture Collection. Murine epithelial ovarian cancer ID8 cells were a gift from K. Roby (Kansas University Medical Center, Kansas City, KS).

Full-length and DN-RAGE cloning and mammalian expression introduction of siRNA and transfection. Full-length RAGE cDNA was generated from lung cDNA (Takara Bio Inc.) and DN RAGE cDNA was generated as previously described (Taguchi et al., 2000). Where indicated, Nucleofector kits for primary SMCs were used (Lonza). RH7777 cells were transfected using lipofectamine 2000 (Invitrogen) according to the manufacturer's protocol. The constructs expressing human full-length, human DN RAGE, or control vector, and siRNAs against LPA1, LPA2, and RAGE, or scramble (negative control; Ambion) were electroporated into primary SMCs using the Nucleofector device according to the manufacturer's protocol (Lonza). After 24 h, cells were stimulated with LPA and subjected to studies.

Colony formation assay. Colony formation assay was performed using the CytoSelect 96-Well Cell Transformation Assay (Cell Biolabs) as per the manufacturer's instructions by plating cells in a layer of 0.4% agarose in DMEM. After 7 d, relative colonies were measured by incubating CyQuant Working Solution and reading the plate in a 96-well fluorometer using a 485/520-nm filter set.

Real-time PCR. RNA was extracted from cells by using RNeasy columns (QIAGEN). cDNA was prepared (Applied Biosystems) and used as a template for quantitative PCR. Primers and probes for murine and rat LPA receptors 1–5 and RAGE were obtained from Applied Biosystems. Gene expression was normalized to the expression of 18S rRNA. Data were analyzed by the $2^{-\Delta\Delta CT}$ method.

Western blot analysis. Total cellular, aorta, or tumor lysates were immunoblotted and probed with LPA1, LPA2, or atx-specific antibodies (Santa Cruz Biotechnology, Inc.), RAGE (Gene Tex), and AKT-specific antibody, p-AKT–specific/total AKT antibody (thr308), p-ERK/total ERK, and p-cyclin D1/total cyclin D1 (Cell Signaling Technology). HRP-conjugated donkey anti–rabbit IgG or HRP-conjugated sheep anti–mouse IgG (GE Healthcare) was used to identify sites of binding of the primary antibody. After probing with the primary antibodies, membranes were stripped of bound immunoglobulins and reprobed with GAPDH (Abcam) or for relative total protein. Blots were scanned with an AlfaImager TM 2200 scanner with AlfaEase (AlfaImager) FC 2200 software. Results are reported as a relative absorbance of test antigen to GAPDH or relative total proteins.

Immunohistochemistry. Acetone-fixed cryostat aortic sections were preincubated with CAS-BLOCK (Invitrogen) for 30 min followed by avidin-biotin block for 15 min. Sections were then subjected to incubation with primary rabbit polyclonal RAGE IgG; Akt and p-Akt (Cell Signaling Technology) overnight at 4°C followed by goat anti–rabbit IgG (Vector Laboratories). Subsequently, Alexa Fluor 555 conjugate (Invitrogen) was incubated for 30 min. After washing, mouse monoclonal smooth muscle actin (Dako) antibody was incubated for 1 h, followed by anti–rat or anti–mouse IgG for 30 min, and then incubated with Alexa Fluor 488 conjugate for 30 min, and finally mounted with 4,6-diamidino-2-phenylindole dihydrochloride (Vector Laboratories). Rabbit IgG (Invitrogen) or omission of the primary antibody was used as a negative control. Slides were mounted with Vectashield mounting media (Vector Laboratories) and observed with an oil immersion objective using a microscope (E800; Nikon). Images were collected using a Radiance 2000 Confocal System and the Lasersharp 2000 software (Bio-Rad Laboratories).

SMC assays. Migration and proliferation assays were performed according to previously published methods (Sakaguchi et al., 2003). SMCs were cultured to 90% confluence. Cells were rinsed with PBS and placed in low serum media (1.5 ml; 0.5–0.1% serum in DMEM) overnight. A scratch line was drawn using a sterile 200 µl pipette tip. Three separate scratch wounds through the cell monolayer moving perpendicular to the line were drawn in the step above. Cells were rinsed with PBS and replaced with 1.5 ml of media containing additives (10 µM LPA or 10 µg/ml S100B final concentration). Photographs were taken after 18 h using phase contrast.

Animal models. All animal experiments were approved by the Institutional Animal Care and Use Committee of Columbia University and New York University and conformed to the guidelines outlined in the National Institutes of Health Guide for Care and Use of Laboratory Animals (National Institutes of Health Pub. No. 85–23, 1996). 4–6-wk-old female C57/BL6 mice (The Jackson Laboratory) were used for studies testing infusion of LPA on vascular signaling and for experiments testing ID8 cells in vivo. Homozygous RAGE-null mice backcrossed >20 generations into C57BL/6 were bred in our laboratory and used as controls for these two sets of studies. Mice were perfused through the left ventricle with 2 ml of sterile PBS to remove all blood. The aorta at the level of the bifurcation of the femoral arteries was cross-clamped and 200 µl of a 100 µM solution of LPA was injected using a 22-gauge needle. Control animals received equal volumes of PBS. At the indicated times after injection, the aorta from the point distal to exit from the left ventricle to the clamp site was rapidly excised and placed in ice-cold buffer. Western blotting for detection of phospho/total Akt and immunohistochemistry to detect phospho-Akt was performed. In the tumor model, mice were injected by the i.p. route with 5×10^6 ID8 cells in 1 ml PBS and LPA was administered daily (100 µmol/liter) in 200 µl PBS or PBS or LPA (100 µmol/liter) in 200 µl PBS and sRAGE (50 µmol/liter) in 200 µl PBS injections for 4 wk. Tumor implantation and development was recorded by counting the numbers and sizes of tumor foci on each organ. In other studies, MMTV-*atx* mice in the FVB genetic background (Liu et al., 2009), provided by G. Mills (University of Texas M.D. Anderson Cancer Center, Houston, TX), were bred into RAGE-null background (backcrossed >12 generations into FVB). RAGE-expressing and RAGE-null MMTV-*atx* littermate mice were sacrificed at 6 wk old and mammary tissue was collected and pooled for analysis by Western blotting.

Data analysis. The mean ± SD is reported. Statistical comparisons among groups were determined using one-way ANOVA. Where indicated, individual comparisons were performed using Student's *t* test.

The authors gratefully acknowledge Dr. Gordon B. Mills for generously sharing the MMTV-*atx* mice (University of Texas M.D. Anderson Cancer Center) and Dr. Katherine Roby for sharing the ID8 cells. The authors gratefully acknowledge the assistance of Ms. Latoya Woods in the preparation of this manuscript.

This work was supported by grants from the U.S. Public Health Service HL60901 and GM62112-S1. S. Chitayat was supported by a Canadian Institutes of Health Research postdoctoral fellowship.

The authors have no competing financial interests.

Submitted: 24 April 2012
Accepted: 23 October 2012

REFERENCES

Bu, D.X., V. Rai, X. Shen, R. Rosario, Y. Lu, V. D'Agati, S.F. Yan, R.A. Friedman, E. Nuglozeh, and A.M. Schmidt. 2010. Activation of the ROCK1 branch of the transforming growth factor-beta pathway contributes to RAGE-dependent acceleration of atherosclerosis in diabetic ApoE-null mice. *Circ. Res.* 106:1040–1051. http://dx.doi.org/10.1161/CIRCRESAHA.109.201103

Cechin, S.R., P.R. Dunkley, and R. Rodnight. 2005. Signal transduction mechanisms involved in the proliferation of C6 glioma cells induced by lysophosphatidic acid. *Neurochem. Res.* 30:603–611. http://dx.doi.org/10.1007/s11064-005-2747-4

Chen, Y., S.S. Yan, J. Colgan, H.P. Zhang, J. Luban, A.M. Schmidt, D. Stern, and K.C. Herold. 2004. Blockade of late stages of autoimmune diabetes by inhibition of the receptor for advanced glycation end products. *J. Immunol.* 173:1399–1405.

Choi, J.W., D.R. Herr, K. Noguchi, Y.C. Yung, C.W. Lee, T. Mutoh, M.E. Lin, S.T. Teo, K.E. Park, A.N. Mosley, and J. Chun. 2010. LPA receptors: subtypes and biological actions. *Annu. Rev. Pharmacol. Toxicol.* 50:157–186. http://dx.doi.org/10.1146/annurev.pharmtox.010909.105753

Chun, J., T. Hla, K.R. Lynch, S. Spiegel, and W.H. Moolenaar. 2010. International Union of Basic and Clinical Pharmacology. LXXVIII. Lysophospholipid receptor nomenclature. *Pharmacol. Rev.* 62:579–587. http://dx.doi.org/10.1124/pr.110.003111

Copeland, J.W., and R. Treisman. 2002. The diaphanous-related formin mDia1 controls serum response factor activity through its effects on actin polymerization. *Mol. Biol. Cell.* 13:4088–4099. http://dx.doi.org/10.1091/mbc.02-06-0092

Dattilo, B.M., G. Fritz, E. Leclerc, C.W. Kooi, C.W. Heizmann, and W.J. Chazin. 2007. The extracellular region of the receptor for advanced glycation end products is composed of two independent structural units. *Biochemistry.* 46:6957–6970. http://dx.doi.org/10.1021/bi7003735

Eng, C.H., T.M. Huckaba, and G.G. Gundersen. 2006. The formin mDia regulates GSK3beta through novel PKCs to promote microtubule

stabilization but not MTOC reorientation in migrating fibroblasts. *Mol. Biol. Cell.* 17:5004–5016. http://dx.doi.org/10.1091/mbc.E05-10-0914

Georas, S.N. 2009. Lysophosphatidic acid and autotaxin: emerging roles in innate and adaptive immunity. *Immunol. Res.* 45:229–238. http://dx.doi.org/10.1007/s12026-009-8104-y

Hofmann, M.A., S. Drury, C. Fu, W. Qu, A. Taguchi, Y. Lu, C. Avila, N. Kambham, A. Bierhaus, P. Nawroth, et al. 1999. RAGE mediates a novel proinflammatory axis: a central cell surface receptor for S100/calgranulin polypeptides. *Cell.* 97:889–901. http://dx.doi.org/10.1016/S0092-8674(00)80801-6

Hudson, B.I., A.Z. Kalea, M. Del Mar Arriero, E. Harja, E. Boulanger, V. D'Agati, and A.M. Schmidt. 2008. Interaction of the RAGE cytoplasmic domain with diaphanous-1 is required for ligand-stimulated cellular migration through activation of Rac1 and Cdc42. *J. Biol. Chem.* 283:34457–34468. http://dx.doi.org/10.1074/jbc.M801465200

Kim, J., J.R. Keys, and A.D. Eckhart. 2006. Vascular smooth muscle migration and proliferation in response to lysophosphatidic acid (LPA) is mediated by LPA receptors coupling to Gq. *Cell. Signal.* 18:1695–1701. http://dx.doi.org/10.1016/j.cellsig.2006.01.009

Kitzing, T.M., A.S. Sahadevan, D.T. Brandt, H. Knieling, S. Hannemann, O.T. Fackler, J. Grosshans, and R. Grosse. 2007. Positive feedback between Dia1, LARG, and RhoA regulates cell morphology and invasion. *Genes Dev.* 21:1478–1483. http://dx.doi.org/10.1101/gad.424807

Koch, M., S. Chitayat, B.M. Dattilo, A. Schiefner, J. Diez, W.J. Chazin, and G. Fritz. 2010. Structural basis for ligand recognition and activation of RAGE. *Structure.* 18:1342–1352. http://dx.doi.org/10.1016/j.str.2010.05.017

Leclerc, E., G. Fritz, M. Weibel, C.W. Heizmann, and A. Galichet. 2007. S100B and S100A6 differentially modulate cell survival by interacting with distinct RAGE (receptor for advanced glycation end products) immunoglobulin domains. *J. Biol. Chem.* 282:31317–31331. http://dx.doi.org/10.1074/jbc.M703951200

Li, H., D. Wang, H. Zhang, K. Kirmani, Z. Zhao, R. Steinmetz, and Y. Xu. 2009. Lysophosphatidic acid stimulates cell migration, invasion, and colony formation as well as tumorigenesis/metastasis of mouse ovarian cancer in immunocompetent mice. *Mol. Cancer Ther.* 8:1692–1701. http://dx.doi.org/10.1158/1535-7163.MCT-08-1106

Lin, M.E., D.R. Herr, and J. Chun. 2010. Lysophosphatidic acid (LPA) receptors: signaling properties and disease relevance. *Prostaglandins Other Lipid Mediat.* 91:130–138. http://dx.doi.org/10.1016/j.prostaglandins.2009.02.002

Liu, S., M. Umezu-Goto, M. Murph, Y. Lu, W. Liu, F. Zhang, S. Yu, L.C. Stephens, X. Cui, G. Murrow, et al. 2009. Expression of autotaxin and lysophosphatidic acid receptors increases mammary tumorigenesis, invasion, and metastases. *Cancer Cell.* 15:539–550. http://dx.doi.org/10.1016/j.ccr.2009.03.027

McIntyre, T.M., A.V. Pontsler, A.R. Silva, A. St Hilaire, Y. Xu, J.C. Hinshaw, G.A. Zimmerman, K. Hama, J. Aoki, H. Arai, and G.D. Prestwich. 2003. Identification of an intracellular receptor for lysophosphatidic acid (LPA): LPA is a transcellular PPARgamma agonist. *Proc. Natl. Acad. Sci. USA.* 100:131–136. http://dx.doi.org/10.1073/pnas.0135855100

Moolenaar, W.H., L.A. van Meeteren, and B.N. Giepmans. 2004. The ins and outs of lysophosphatidic acid signaling. *Bioessays.* 26:870–881. http://dx.doi.org/10.1002/bies.20081

Pamuklar, Z., L. Federico, S. Liu, M. Umezu-Goto, A. Dong, M. Panchatcharam, Z. Fulkerson, E. Berdyshev, V. Natarajan, X. Fang, et al. 2009. Autotaxin/lysopholipase D and lysophosphatidic acid regulate murine hemostasis and thrombosis. *J. Biol. Chem.* 284:7385–7394. http://dx.doi.org/10.1074/jbc.M807820200

Panchatcharam, M., S. Miriyala, F. Yang, M. Rojas, C. End, C. Vallant, A. Dong, K. Lynch, J. Chun, A.J. Morris, and S.S. Smyth. 2008. Lysophosphatidic acid receptors 1 and 2 play roles in regulation of vascular injury responses but not blood pressure. *Circ. Res.* 103:662–670. http://dx.doi.org/10.1161/CIRCRESAHA.108.180778

Park, L., K.G. Raman, K.J. Lee, Y. Lu, L.J. Ferran Jr., W.S. Chow, D. Stern, and A.M. Schmidt. 1998. Suppression of accelerated diabetic atherosclerosis by the soluble receptor for advanced glycation endproducts. *Nat. Med.* 4:1025–1031. http://dx.doi.org/10.1038/2012

Roby, K.F., C.C. Taylor, J.P. Sweetwood, Y. Cheng, J.L. Pace, O. Tawfik, D.L. Persons, P.G. Smith, and P.F. Terranova. 2000. Development of a syngeneic mouse model for events related to ovarian cancer. *Carcinogenesis.* 21:585–591. http://dx.doi.org/10.1093/carcin/21.4.585

Sakaguchi, T., S.F. Yan, S.D. Yan, D. Belov, L.L. Rong, M. Sousa, M. Andrassy, S.P. Marso, S. Duda, B. Arnold, et al. 2003. Central role of RAGE-dependent neointimal expansion in arterial restenosis. *J. Clin. Invest.* 111:959–972.

Shang, L., R. Ananthakrishnan, Q. Li, N. Quadri, M. Abdillahi, Z. Zhu, W. Qu, R. Rosario, F. Touré, S.F. Yan, et al. 2010. RAGE modulates hypoxia/reoxygenation injury in adult murine cardiomyocytes via JNK and GSK-3beta signaling pathways. *PLoS ONE.* 5:e10092. http://dx.doi.org/10.1371/journal.pone.0010092

Smyth, S.S., H.Y. Cheng, S. Miriyala, M. Panchatcharam, and A.J. Morris. 2008. Roles of lysophosphatidic acid in cardiovascular physiology and disease. *Biochim. Biophys. Acta.* 1781:563–570. http://dx.doi.org/10.1016/j.bbalip.2008.05.008

Taguchi, A., D.C. Blood, G. del Toro, A. Canet, D.C. Lee, W. Qu, N. Tanji, Y. Lu, E. Lalla, C. Fu, et al. 2000. Blockade of RAGE-amphoterin signalling suppresses tumour growth and metastases. *Nature.* 405:354–360. http://dx.doi.org/10.1038/35012626

Touré, F., G. Fritz, Q. Li, V. Rai, G. Daffu, Y.S. Zou, R. Rosario, R. Ramasamy, A.S. Alberts, S.F. Yan, and A.M. Schmidt. 2012. Formin mDia1 mediates vascular remodeling via integration of oxidative and signal transduction pathways. *Circ. Res.* 110:1279–1293. http://dx.doi.org/10.1161/CIRCRESAHA.111.262519

Valentine, W.J., Y. Fujiwara, R. Tsukahara, and G. Tigyi. 2008. Lysophospholipid signaling: beyond the EDGs. *Biochim. Biophys. Acta.* 1780:597–605. http://dx.doi.org/10.1016/j.bbagen.2007.08.008

Xu, Y., F. Toure, W. Qu, L. Lin, F. Song, X. Shen, R. Rosario, J. Garcia, A.M. Schmidt, and S.F. Yan. 2010. Advanced glycation end product (AGE)-receptor for AGE (RAGE) signaling and up-regulation of Egr-1 in hypoxic macrophages. *J. Biol. Chem.* 285:23233–23240. http://dx.doi.org/10.1074/jbc.M110.117457

Xue, J., V. Rai, D. Singer, S. Chabierski, J. Xie, S. Reverdatto, D.S. Burz, A.M. Schmidt, R. Hoffmann, and A. Shekhtman. 2011. Advanced glycation end product recognition by the receptor for AGEs. *Structure.* 19:722–732. http://dx.doi.org/10.1016/j.str.2011.02.013

Yan, S.F., R. Ramasamy, and A.M. Schmidt. 2010. The RAGE axis: a fundamental mechanism signaling danger to the vulnerable vasculature. *Circ. Res.* 106:842–853. http://dx.doi.org/10.1161/CIRCRESAHA.109.212217

Zhou, Z., K. Wang, M.S. Penn, S.P. Marso, M.A. Lauer, F. Forudi, X. Zhou, W. Qu, Y. Lu, D.M. Stern, et al. 2003. Receptor for AGE (RAGE) mediates neointimal formation in response to arterial injury. *Circulation.* 107:2238–2243. http://dx.doi.org/10.1161/01.CIR.0000063577.32819.23